# IMPACT LOAD-DEFORMATION PROPERTIES OF PILE CUSHIONING MATERIALS

by

T. J. Hirsch
Associate Research Engineer

and

Thomas C. Edwards
Assistant Research Engineer

*Research Report Number 33-4*
*Piling Behavior*
*Research Project Number 2-5-62-33*

**Sponsored by**
**The Texas Highway Department**
**in Cooperation with the**
**U. S. Department of Commerce, Bureau of Public Roads**

**May, 1966**

**TEXAS TRANSPORTATION INSTITUTE**
**Texas A&M University**
**College Station, Texas**

# TABLE OF CONTENTS

# LIST OF FIGURES

# LIST OF TABLES

# FOREWORD

The information contained herein was developed on Research Project 2-5-62-33 entitled "Piling Behavior" which is a cooperative research project sponsored jointly by the Texas Highway Department and U. S. Department of Commerce, Bureau of Public Roads. The broad objective of this project is to fully develop the use of the computer solution of the wave equation so that it may be used to predict driving stresses in piling and be used to estimate the static load bearing capacity of piling from driving resistance records. This report covers the specific objective of determining the dynamic load-deformation properties of various pile cushion materials. These properties are necessary for the wave equation analysis and have been found to have a most significant effect on the driving stresses and pile penetration during driving.

# *Impact Load-Deformation Properties of Pile Cushioning Materials*

## Chapter I

### INTRODUCTION

1.1 *Cushion Purpose.* In pile driving it is frequently necessary to include a cushioning material between the helmet and striking ram and also between the head of the pile and helmet. In concrete piles, both reinforced and prestressed, it is necessary to have cushioning material between the helmet and head of the pile to prevent spalling of the concrete. The cushion serves the following purposes:

1. Distributes the impact load uniformly over the surface of the pile head.

2. Eliminates stress concentrations caused by pile head irregularities.

3. Attenuates the impulsive force of the ram so that the stress introduced into the pile does not exceed fracture or yield stress.

4. Controls or increases the impact time which has an important effect on the penetration of the pile.

1.2 *Influence of Cushion Stiffness on Pile Stresses.* In order to illustrate the effect of cushion load-deformation characteristics on stresses in piles struck by a falling ram, consider the following ideal situation.

A long elastic rod, with an elastic cushion on top is struck by a falling ram as shown in Figure 1. By using the basic differential equation for waves in prismatic bars and the boundary conditions imposed by the continuity of the ram displacement, cushion compression, and pile head displacement, equations for the compressive stress at the head of the pile can be developed.[4]* Omitting the mathematics, the approximate equations for the maximum compressive stress at the pile head are as follows:

Notations used are:

$\sigma_{max}$ = maximum compressive stress at pile head in psi

$W$ = ram weight in lb

$V$ = ram impact velocity in in./sec

$= \sqrt{2gh}$

$h$ = ram free fall in in.

$g$ = acceleration due to gravity, 386 in./sec$^2$

$e$ = Napierian base, 2.71828

$K$ = cushion stiffness in lb/in.

$= \dfrac{A_c E_c}{t_c}$

$A_c$ = cross-sectional area of cushion in in.$^2$

$E_c$ = modulus of elasticity of cushion in psi

$t_c$ = initial uncompressed thickness of cushion in in.

$t$ = time in sec.

$A$ = cross-sectional area of pile in in.$^2$

$E$ = modulus of elasticity of pile in psi

$\gamma$ = unit weight of pile in lb/in.$^3$

$n = \dfrac{K}{2A}\sqrt{\dfrac{g}{E\gamma}}$

$p = \sqrt{\dfrac{Kg}{W}}$

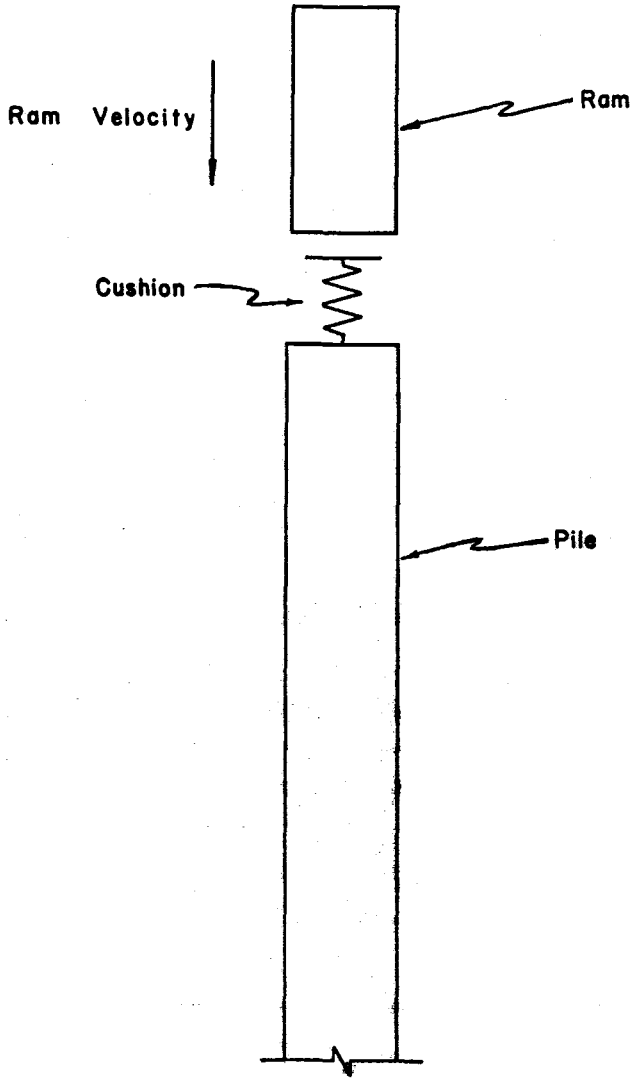


*Figure 1. Idealized ram, cushion, and pile system.*

*Superscript numbers refer to corresponding references in Reference List.

Case I. $n < p$

$$\sigma max = \frac{-KV}{A\sqrt{p^2-n^2}} e^{-nt} \sin (t\sqrt{p^2-n^2}) \qquad \text{Eq. 1}$$

where t is found from the expression

$$\tan (t\sqrt{p^2-n^2}) = \frac{\sqrt{p^2-n^2}}{n}$$

Case II. $n = p$

$$\sigma max = -\left(\frac{KV}{nA} - \frac{W}{A}\right) e^{-1} \qquad \text{Eq. 2}$$

Case III. $n > p$

$$\sigma max = -\frac{KV}{A\sqrt{n^2-p^2}} e^{-nt} \sinh (t\sqrt{n^2-p^2}) \qquad \text{Eq. 3}$$

where t is found from the expression

$$\tanh (t\sqrt{n^2-p^2}) = \frac{\sqrt{n^2-p^2}}{n}$$

Equations 1, 2, or 3 can be used to determine the maximum compressive stress at the pile head. For most practical pile problems n will be less than p and Equation 1 will be used. However, this is not always the case. For a given pile these equations could be used to determine a desirable combination of ram weight W, ram velocity V, and cushion stiffness K so as not to exceed a given allowable compressive stress at the pile head.

To illustrate the use of the equations consider the following situation which was used in a laboratory pile test.

Given:

15 in. square prestressed concrete pile
65 ft long
$A = 225$ in.$^2$
$\gamma = 0.0875$ lb/in.$^3$
$E = 7.15 \times 10^6$ psi

Green oak cushion, grain horizontal

$A_c = 225$ in.$^2$
$E_c = 15{,}000$ psi
$t_c = 3.5$ in.
$K = \frac{A_c E_c}{t_c} = 960{,}000$ lb/in.

Steel ram

$W = 2128$ lb
$h = 36$ in.
$V = \sqrt{2gh} = 167$ in./sec
$g = 386$ in./sec$^2$

Calculations:

$$n = \frac{K}{2A}\sqrt{\frac{g}{E\gamma}} = 53 \text{ sec}^{-1}$$

$$p = \sqrt{\frac{Kg}{W}} = 417 \text{ sec}^{-1}$$

Since $n < p$ Eq. 1 of Case I applies.

$$\tan (t\sqrt{p^2-n^2}) = \frac{\sqrt{p^2-n^2}}{n} = \frac{414}{53} = 7.8$$

so $t\sqrt{p^2-n^2} = 82.7°$ or 1.44 radians
$t = .00348$ sec

Using Eq. 1

$$\sigma max = \frac{-KV}{A\sqrt{p^2-n^2}} e^{-nt} \sin (t\sqrt{p^2-n^2})$$

$$= \frac{-960{,}000 \times 167\ e^{-53 \times .00348}}{225 \times 414} \sin 82.7°$$

$\sigma max = 1420$ psi

Values of the maximum compressive stress for different cushion thickness are shown in Table 1. Table 1 also compares the calculated values with those obtained from strain gage measurements on this pile, ram and cushion system. These pile tests were conducted in the Structural Research Laboratory at the Texas A&M Research Annex. The pile was suspended horizontally and struck by the ram swinging as a pendulum.

The significant effect of the cushion stiffness on the pile stress is shown by Table 1. Similar results are shown by Table 2. The pile used in developing the values in Table 2 was of lightweight aggregate concrete which had a lower modulus of elasticity and lower density. It can be noted by comparing values in Tables 1 and 2 that the less stiff, lightweight concrete, pile has smaller stresses than those in the conventional concrete pile.

1.3 *Influence of Cushion Stiffness on Permanent Set of Pile.* In order for a pile to penetrate under one blow of the hammer the impulsive force transmitted by the ram-cushion system must be of sufficient magnitude to overcome the inertia of the pile as well as yield the soil along the side of the pile and at the point. Once this condition has been met, the penetration of the pile is dependent upon the duration and excess magnitude of the force impulse. If the driving energy is held constant, the hammer impulse force duration will increase as the ram weight increases and/or cushion stiffness decreases. Therefore, the penetration of the pile per blow will usually increase as the impulse force duration increases. This observation is illustrated in Figure 2 which presents results from a Wave Equation analysis.[1]

It should be kept in mind, that if the cushion is too soft to develop an impulse force of sufficient magnitude to get the pile moving, using a softer cushion will not increase the pile penetration. This condition may arise when extremely hard driving (soil) resistance is encountered.

TABLE 1. EFFECT OF CUSHION THICKNESS ON MAXIMUM COMPRESSIVE STRESS AT PILE HEAD

(Prestressed concrete pile 15 in. square by 65 ft long, ram weight 2128 lb, fall 36 in., and fresh green oak cushion with $E_c$=15,000 psi and $A_c$=225 in.$^2$ as in example problem)

Class "F" Concrete, E=7,150,000 psi, $\gamma = 0.0875$ lb/in.$^3$

| Green Oak Cushion thickness in inches | Maximum Compressive Stress at Pile Head in psi | |
|---|---|---|
| | Calculated by Eq. 1 | Experimental Strain Gage Measurement |
| 3.5 | −1420 | −1400 |
| 5.5 | −1170 | −1370 |
| 7.5 | −1020 | −1210 |
| 9.5 | − 920 | − 850 |

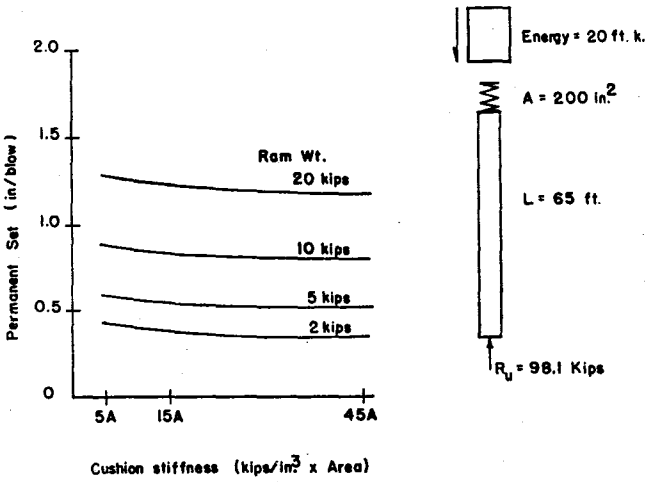


*Figure 2. Effect of cushion stiffness and ram weight on permanent set when driving energy is held constant.*

1.4 *Influence of Cushion Coefficient of Restitution on Piling Behavior.* When a pile cushion is loaded and unloaded by a pile driver ram's impact the cushion stress-strain curve has a characteristic hysteresis loop as shown in Figure 3b. From this hysteresis characteristic it is apparent that energy is dissipated in the cushion as heat. In pile driving terminology the term "coefficient of restitution" (u) has been used to describe this amount of energy dissipation when the ram impacts a pile.

Figure 3 shows 2 methods of determining the value u for cushion materials. By basic definition the coefficient of restitution is defined as the ratio obtained by dividing the relative velocity of two impacting bodies after impact by their relative velocity before impact. Thus as shown in Figure 3a

$$u = -\frac{V_2}{V_1}$$

and it follows that

$$u = \sqrt{\frac{h_2}{h_1}}$$

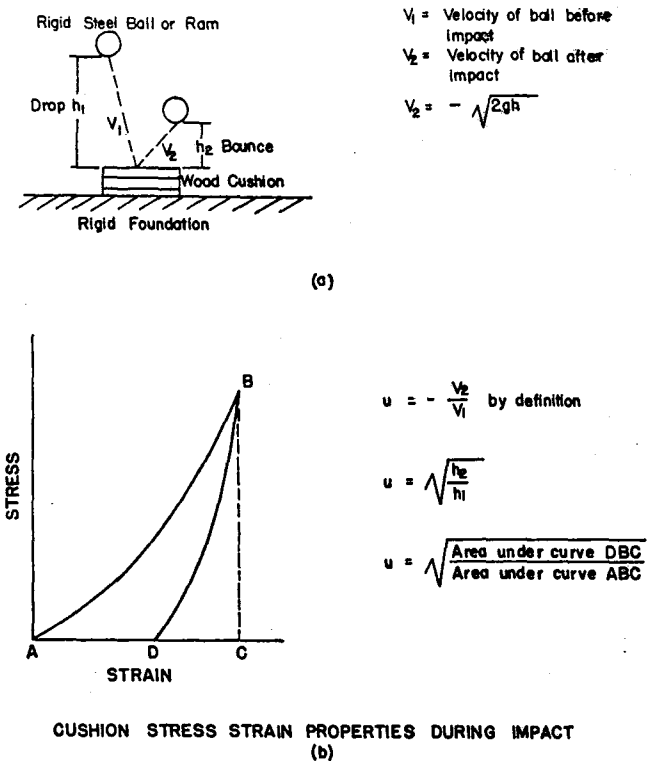


*Figure 3. Coefficient of restitution property of cushion material.*

The value of u can also be computed from the data in Figure 3b which shows the stress strain properties of the cushion during impact.

$$u = \sqrt{\frac{\text{Area under curve DBC}}{\text{Area under curve ABC}}}$$

A perfectly elastic cushion will have a $u = 1.0$ while a perfectly plastic one will have a $u = 0$. The value of u is most significant in determining how much driving energy is transmitted to the pile.

# Chapter II

## BEHAVIOR OF WOOD UNDER IMPACT COMPRESSIVE LOAD PERPENDICULAR TO THE GRAIN

2.1 *General.* In the previous chapter an attempt was made to show the significance of cushion properties on the behavior of piling during driving. Initial attempts to apply the wave equation analysis for predicting driving stresses and pile displacements did not correlate well with field tests. This was due primarily to very poor estimates of the modulus of elasticity and other stress-strain properties of the wood cushioning material used. Consequently a program was set up to determine the stress-strain properties of certain types of wood cushions under impact loads from a pile driver ram. It was also desired to determine how the stress-strain properties changed under repeated blows from the pile driver ram.

2.2 *Cushion Testing Program.* The materials investigated are broken into two groups, woods and synthetics, as follows:

1. Woods
   a. Pine Plywood—¾ in. white pine 5 ply with sanded faces, structural grade A2, purchased commercially.
   b. Fir Plywood—¾ in. Douglas fir 3 ply with sanded faces, structural grade AB, purchased commercially.
   c. Gum Plank—2 in. x 8 in., dressed gum of unknown type, obtained from the Austin Bridge Co.

d. Green Oak—2 in. x 8 in., rough cut, structural grade No. 2 or Btr., obtained commercially.

2. Synthetics

a. Micarta—a thermosetting plastic made from fabric, paper or wood veneers impregnated with phenol-formaldehyde resins and compressed under heat into a permanently solid substance. Obtained from the Raymond International Co. Available commercially from the Westinghouse Co.

b. Garlock Asbestos Packing—Asbestos impregnated with graphite. Obtained from the Austin Bridge Co.

The testing program was broken into two phases. The first phase consisted of determining the properties of the wood cushions under impact load. The results of these tests are compared with data from static compression tests. The second phase discussed, in Chapter III, consisted of performing cyclic static loads on the cushions.

2.3 *Impact Testing Procedure.* The cushion dimensions, ram weight, and fall are shown in Table 3. The cushions were mounted in a test apparatus, as shown in Figure 4, in a laterally unconfined condition. This condition was chosen to simulate cushion conditions used on full scale pile test conducted in the laboratory. Under field pile driving conditions the cushion may or may not have some lateral confinement depending on the helmet or driving head used.

The specimens were tested by dropping the ram from the specified height (usually 3 ft) and recording the accelerometer reading on an oscillograph. Accelerometer data were recorded on the first blow and at twenty-blow increments thereafter. From the accelerometer trace shown in Figure 5 both the load and deformation of the wood cushion could be determined.

2.4 *Instrumentation.* The instrumentation consisted of the following:

a. Endevco Model 2211C piezoelectric accelerometer

b. Endevco Model 2614 B accelerometer amplifier

c. Honeywell Visicorder No. 1508 (Recording oscillograph)

d. Honeywell Galvanometer M400-120

TABLE 2. EFFECT OF CUSHION THICKNESS ON MAXIMUM COMPRESSIVE STRESS AT PILE HEAD
(Prestressed concrete pile 15 in. square by 65 ft long, ram weight 2128 lb, fall 36 in., and fresh green oak cushion with $E_c$=15,000 psi and $A_c$=225 in.$^2$)
Class "Y" Concrete, E=3,960,000 psi, $\gamma$ = 0.0715 lb/in.$^3$

| Green Oak Cushion thickness in inches | Maximum Compressive Stress at Pile Head in psi | |
|---|---|---|
| | Calculated by Eq. 1 | Experimental Strain Gage Measurement |
| 3.5 | −1280 | −1280 |
| 5.5 | −1090 | −1100 |
| 7.5 | − 965 | −1080 |
| 9.5 | − 860 | − 620 |

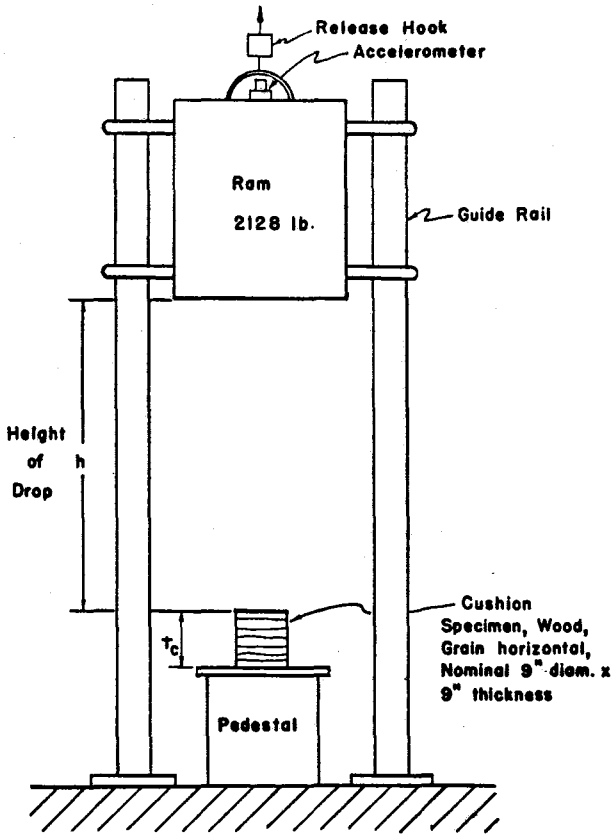


*Figure 4. Impact test apparatus.*

The accelerometer was mounted on the top surface of the ram with an insulated mounting stud. The output of the accelerometer, due to the decelerations of the ram at impact, was amplified and recorded as decelerations on the Visicorder. The gain of the amplifier could be varied to give g scales of 1 in. = 100g, 3 in. = 100g, and 10 in. = 100g. For most tests, 3 in. = 100g was used with a paper speed of 80 in./sec. Time lines were placed on the record paper in 0.01 sec intervals.

2.5 *Data Reduction.* The data needed to determine the desired behavior of the wood cushions are those of stress and strain. This information was obtained from the ram accelerometer trace. A typical accelerometer trace is illustrated by Figure 5. The force on the cushion at any time T after initial contact is

$$F = Ma$$

where F = force on cushion in lb at time T
M = mass of ram in lb-sec$^2$/ft
a = accelerometer reading in ft/sec$^2$ at time T

The velocity $V_1$ of the ram at impact with the cushion is

$$V_1 = \sqrt{2gh}$$

where h = ram fall in in.

The velocity of the ram at any time T is then equal to

$$V = V_1 - \int_{t=0}^{t=T} a\, dt \qquad \text{Eq. 4}$$

Since the head of the ram is in contact with the head of the cushion at time t=0, the displacement of the cushion head at any time T can be found by

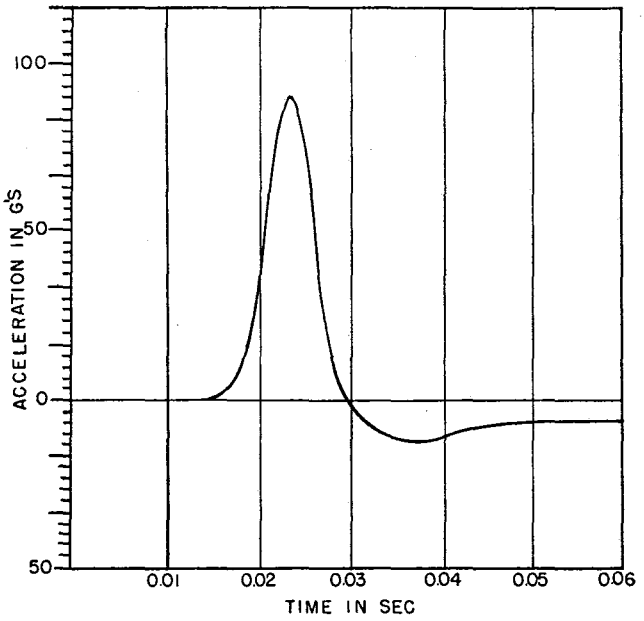


*Figure 5. Typical accelerometer trace.*

$$S = \int_{t=0}^{t=T} V\,dt \qquad \text{Eq. 5}$$

Equations 4 and 5 are numerically integrated to find the velocity V and deformation S of the cushion. Figure 6 shows typical results. The data from the accelerometer trace were transposed to IBM punch cards and the calculations for velocity and displacement were performed by an IBM 7094 digital computer.

The cushion stress $\sigma_c$ at any time T is determined by

$$\sigma_c = \frac{F}{A_c} \qquad \text{Eq. 6}$$

where $A_c$ = cross-sectional area of cushion in in.$^2$ and the nominal cushion strain $(\epsilon_c)$, at any time T was, determined by

$$\epsilon_c = \frac{S}{t_c} \qquad \text{Eq. 7}$$

where $t_c$ = initial uncompressed cushion thickness. Permanent cushion deformation (or strain) is not included in the nominal strain reported in this Chapter. This was done because the main interest is only in the stiffness of the cushion K (load-deformation property) under a ram blow. By definition

$$K = \frac{F}{S} \text{ in lb/in.}$$

Using equations 6 and 7 yields

$$K = \frac{A_c \sigma_c}{t_c \epsilon_c} \qquad \text{Eq. 8}$$

The modulus of elasticity of wood as used in this paper corresponds to a "secant" modulus of elasticity and is

$$E_c = \frac{\sigma_c}{\epsilon_c} \qquad \text{Eq. 9}$$

Introducing Eq. 9 into Eq. 8 yields

$$K = \frac{A_c E_c}{t_c}$$

This is the definition of K as given in Chapter I.

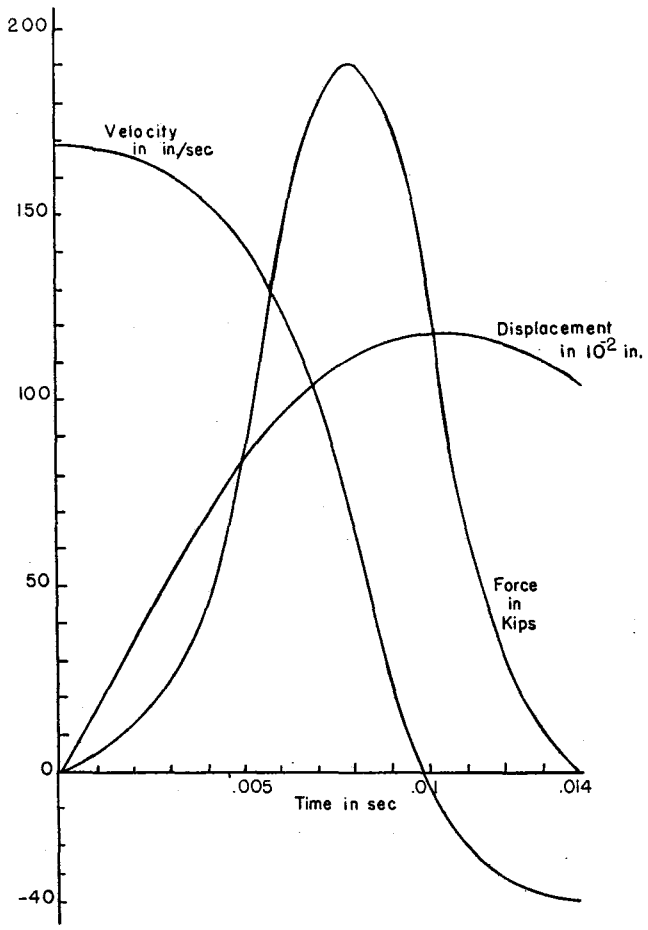


*Figure 6. Typical cushion force and displacement vs. time computed from accelerometer trace. Ram velocity also shown.*

In this Chapter it is desired to investigate the stress-strain characteristics of wood cushions and to determine suitable values of the Secant Modulus of Elasticity $E_c$ for wood compressed by stress perpendicular to the grain.

2.6 *Test Results and Observations.* During the first several blows of the pile ram the wood cushions

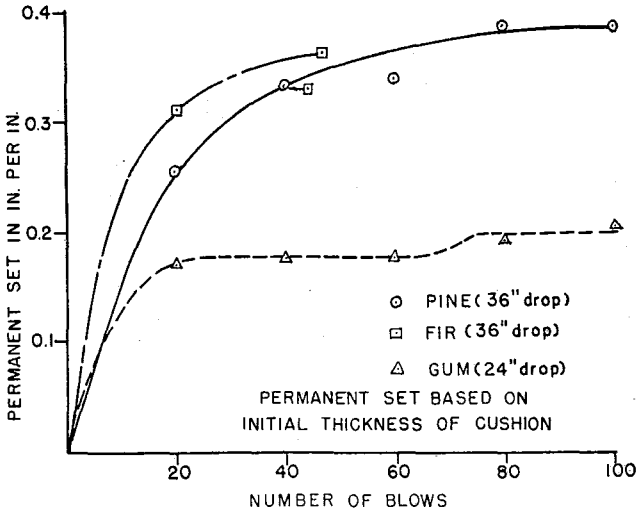


*Figure 7. Permanent set vs. number of blows.*

TABLE 3. PERTINENT WOOD CUSHION DATA

| Cushion Mat'l. | Diameter in. | Thickness in. | Ram wt. lb | Height of Drop in. |
|---|---|---|---|---|
| ¾" Fir Plywood | 9 | 9 | 2128 | 36 |
| ¾" Pine Plywood | 9 | 9 | 2128 | 36 |
| 2" Gum Plank | 8.68 | 8.2 | 2128 | 24 |

attained a considerable amount of permanent deformation or set. Figure 7 shows how the permanent set increased as the number of blows increased. After approximately 20 blows the Gum wood (a hardwood) tended to stabilize at a permanent set of about 0.19 in./in. The laminated plywoods of pine and fir (softwoods) eventually stabilized after about 40 blows with a permanent set of about 0.38 in./in. Before this relatively stable condition was reached, the stress-strain properties of the wood changed at each blow. The stress-strain properties finally stabilized, however at the upper limit of consolidation. The consolidation limit is probably a function of the impact energy for a given ram weight. Undoubtedly these cushions could be consolidated further under higher impact energies; i.e. by using a heavier ram and/or a larger stroke.

Figure 8 shows how the maximum ram acceleration increased under the first several blows and also how the impulse duration decreased. It should be noted that the ram acceleration finally stabilized after approximately 40 blows, for the laminated plywoods of Pine and Fir.

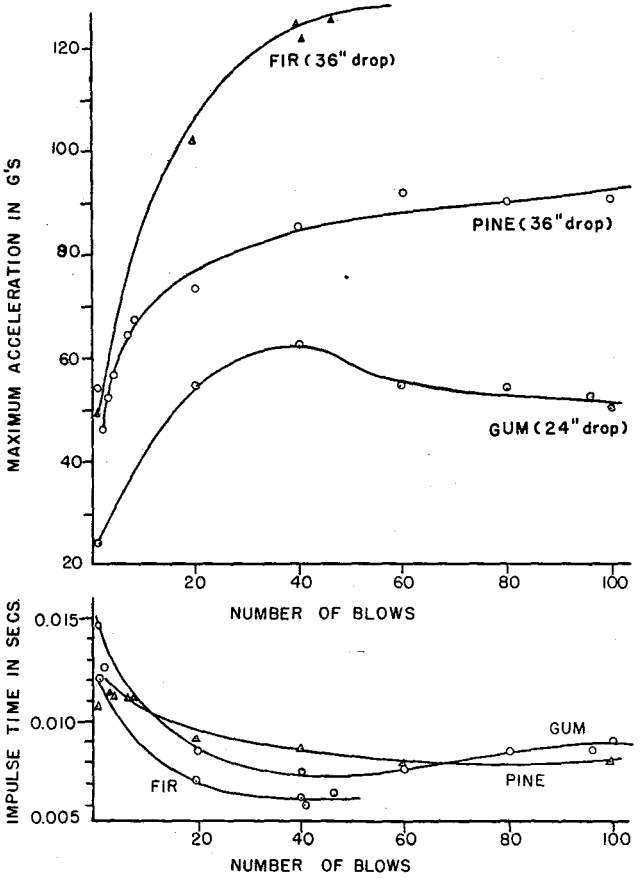


*Figure 8. Maximum acceleration and impulse time vs. number of blows.*

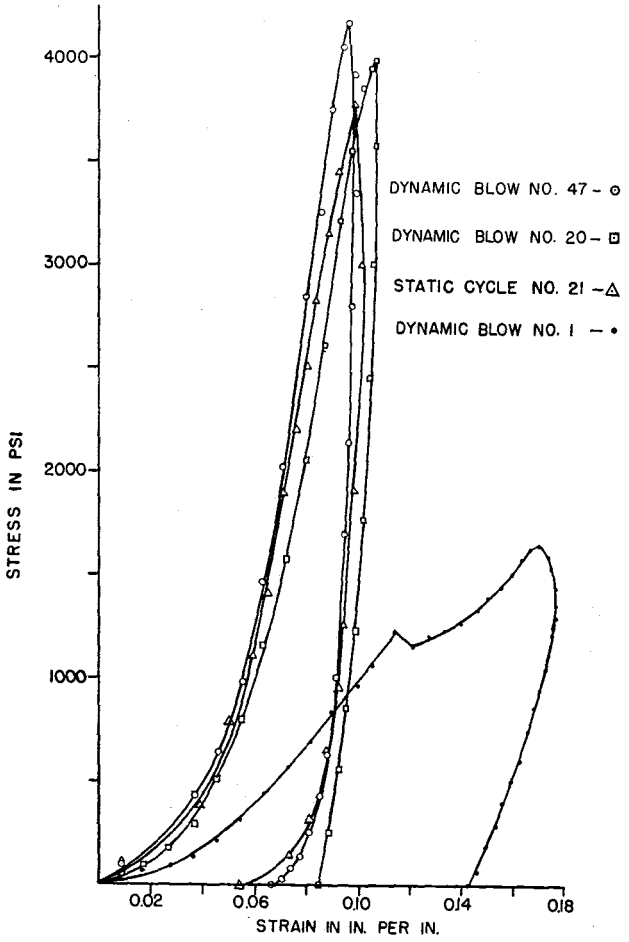


*Figure 9. Stress vs. strain for Fir cushion.*

The Gum wood on the other hand exhibited a drop off in ram acceleration as the blows increased past 40. After 40 blows the Gum cushion split in a vertical direction and sections along the periphery actually separated from the specimen. This indicated that in an unconfined condition the Gum or hardwood cushion could not absorb the amount of energy used in these tests. This effect was also observed in the Oak cushions tested. Because of these splitting failures the impact testing of the Oak cushions was discontinued. Static tests were run on the Oak cushions.

Figures 9, 10, and 11 show typical impact stress-strain curves for the Fir Plywood, Pine Plywood, and Gum cushions respectively. Included on Figures 9 and 10 is a static stress-strain curve obtained by loading each of the specimens in a hydraulic testing machine at a slow rate. The static curves were presented to illustrate the remarkable similarity both qualitatively and quantitatively.

Figure 9 also shows the impact stress-strain relationship of the Fir Plywood under the first blow. After about 20 blows the stress-strain relationship began to stabilize. Similar observations are also illustrated by Figure 10 for the Pine Plywood.

In Chapter I theoretical equations were presented which could be used to calculate the maximum driving compressive stress at the head of a pile. In the development of these equations it was assumed that the wood

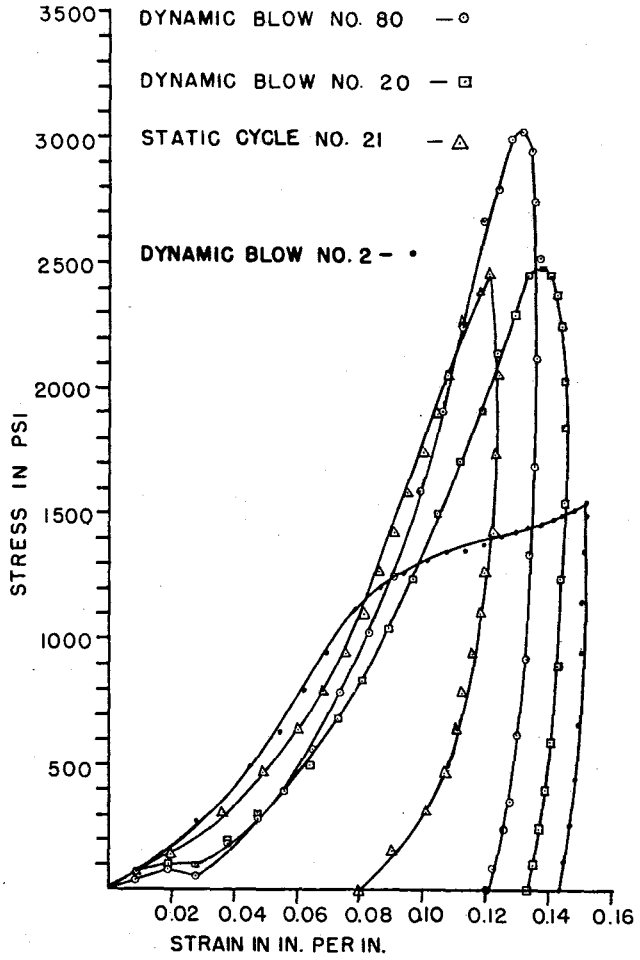


*Figure 10. Stress vs. strain for Pine cushion.*

cushion was an elastic material with an elastic modulus $E_c$. It can be seen from the data in Figures 9, 10, and 11 that this is not exactly the case. Equations 1, 2, or 3 can be used to calculate the driving stresses with reasonable accuracy however, if one is prudent in choosing a Secant Modulus of Elasticity of the wood cushion in the desired condition and at the desired stress level. To aid in making a reasonable choice of $E_c$, Tables 4, 5, and 6 present Secant Moduli of Elasticity value of the Fir Plywood, Pine Plywood, and Gum cushions tested.

TABLE 4. SECANT MODULI OF ELASTICITY OF FIR PLYWOOD CUSHION MATERIAL UNDER IMPACT LOAD PERPENDICULAR TO GRAIN

| Stress Level in psi | Secant Modulus of Elasticity, $E_c$ in psi | | | |
|---|---|---|---|---|
| | Blow 1 | Blow 20 | Blow 47 | Static Test After Blow 20 |
| 500 | 7,150 | 10,900 | 12,500 | 11,600 |
| 1000 | 9,900 | 17,000 | 17,900 | 17,600 |
| 1500 | 9,400 | 21,400 | 23,400 | 22,400 |
| 2000 | | 25,600 | 27,800 | 27,000 |
| 2500 | | 29,800 | 32,100 | 31,300 |
| 3000 | | 33,300 | 36,600 | 34,400 |
| 3500 | | 36,500 | 39,800 | 37,600 |
| 4000 | | | 43,000 | |

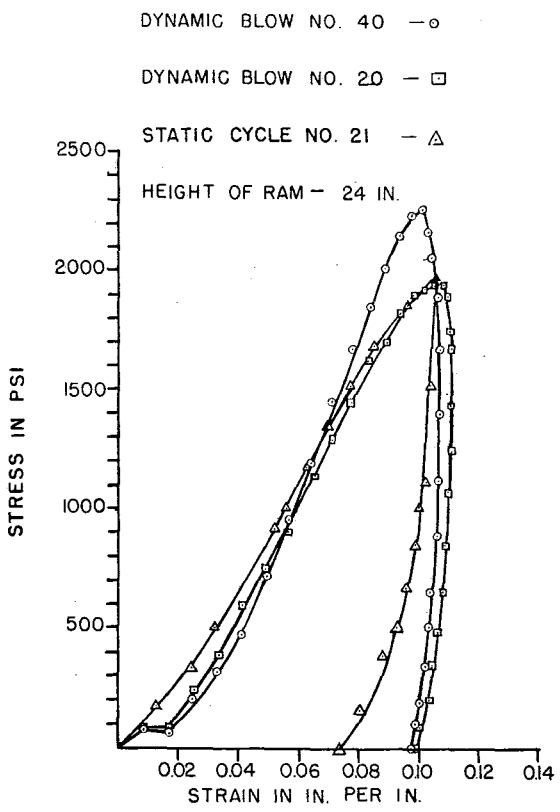


*Figure 11. Stress vs. strain for Gum cushion.*

Values are given at different degrees of consolidation (indicated by Blow No.) and at different stress levels.

In using simplified dynamic pile driving formulas to predict the bearing capacity of a pile from the pile penetration per blow and in using the computer wave equation analysis, it is desirable to know the coefficient of restitution of the cushion material. Coefficient of restitution values were determined from the test data by dividing the ram velocity immediately after impact by the ram velocity before impact

$$u = -\frac{V_2}{V_1}$$

where $u$ = coefficient of restitution
$V_1$ = ram velocity before impact
$V_2$ = ram velocity after impact

TABLE 5. SECANT MODULI OF ELASTICITY OF PINE PLYWOOD CUSHION MATERIAL UNDER IMPACT LOAD PERPENDICULAR TO GRAIN

| Stress Level in psi | Secant Modulus of Elasticity, $E_c$ in psi | | | |
|---|---|---|---|---|
| | Blow 2 | Blow 20 | Blow 80 | Static Test After Blow 20 |
| 500 | 11,100 | 8,000 | 8,000 | 9,600 |
| 1000 | 13,900 | 11,400 | 12,200 | 12,800 |
| 1500 | 10,300 | 14,200 | 15,300 | 16,300 |
| 2000 | | 16,400 | 18,500 | 18,900 |
| 2500 | | | 21,200 | |
| 3000 | | | 23,300 | |

TABLE 6. SECANT MODULI OF ELASTICITY OF GUM WOOD CUSHIONING MATERIAL UNDER IMPACT LOAD PERPENDICULAR TO GRAIN

| Stress Level in psi | Secant Modulus of Elasticity, $E_c$ in psi | | |
|---|---|---|---|
| | Blow 20 | Blow 40 | Static Test After Blow 20 |
| 500 | 13,200 | 12,000 | 15,600 |
| 1000 | 17,000 | 17,000 | 18,200 |
| 1500 | 18,800 | 20,300 | 19,800 |
| 2000 | 18,700 | 22,700 | 19,000 |
| 2500 | | 25,000 | |

Figure 12 shows that u tends to increase up to about blow number 20 in the case of the Fir and Pine Plywoods. The Gum wood tended to split and u did not increase significantly. The u values for Oak were estimated on the basis of only 2 tests and are only indicative of its probable value. It should be remembered that the cushions tested in this investigation were not laterally confined. If a cushion is laterally confined the u values will probably be greater than these.

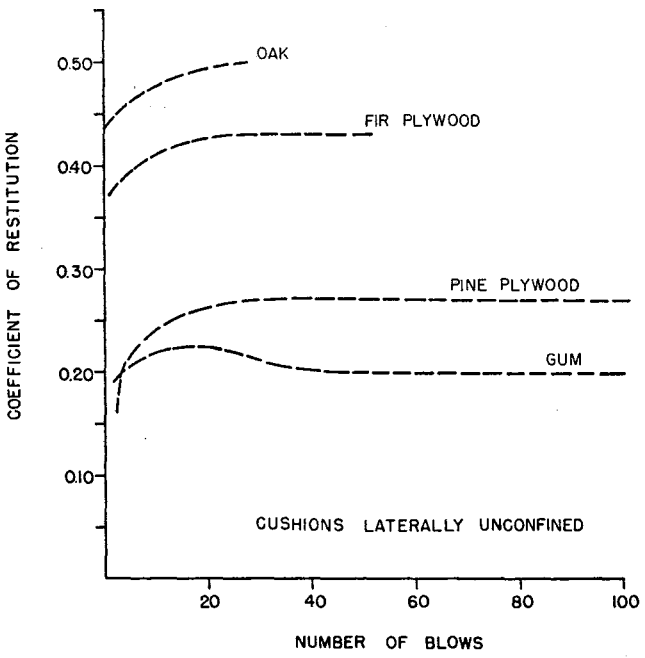


*Figure 12. Average impact coefficient of restitution values for different blow numbers.*

# Chapter III

## BEHAVIOR OF OAK, MICARTA, AND ASBESTOS MATERIALS UNDER STATIC LOADS

3.1 *General.* In the previous chapter it was shown that the static stress-strain curves of the wood materials agreed remarkably well with the stress-strain curve under impact load. It is the purpose of this chapter to describe the static load test method and to present stress-strain data on certain other materials which are used for pile cushioning and capblocks.

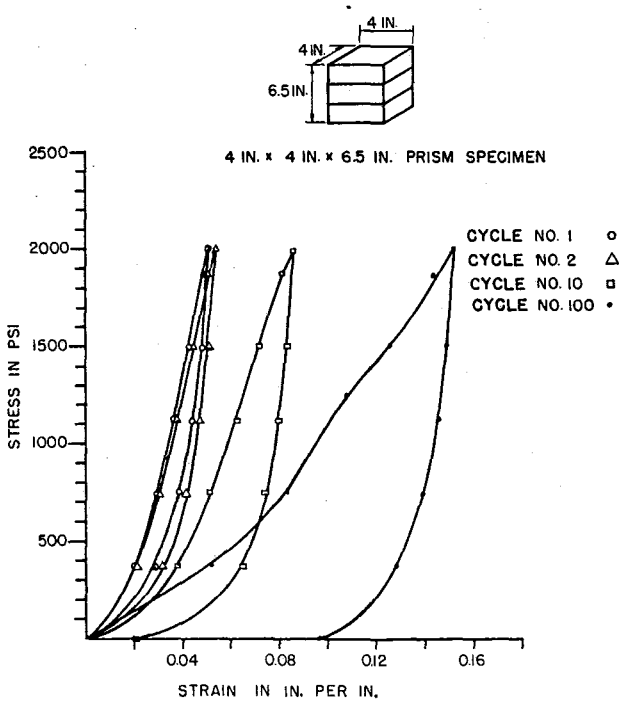


*Figure 13. Stress vs. strain for Oak cushion specimen.*

3.2 *Static Load Test Procedure.* The test specimens were loaded in a universal testing machine and the deformations were measured with 3 Ames dial gages capable of reading 0.001 in. of deformation. The 3 Ames dial gages were positioned at 0°, 120°, and 240° locations around the testing machine loading head. The load was gradually applied in several increments as indicated by the data points on the stress-strain figures. At each load increment the load was maintained for several seconds until the Ames dial gages stabilized at a relatively constant deformation reading. These dial gage readings and total load were recorded and then the next increment of load was applied and the procedure repeated. After the desired peak load was reached, the specimens were unloaded by decreasing the load in several increments. At each increment of load and the unloading cycle, the load was maintained for several seconds until the dial gages stabilized at a relatively constant reading. These dial gage readings and total load were recorded before proceeding with the next increment of unloading.

In the case of the Oak and Asbestos materials, the loading and unloading cycles were repeated for a large number of times in order to observe the mechanical conditioning of the material. Usually after about 10 to 20 cycles the material became consolidated and obtained relatively stable stress-strain characteristics similar to those obtained under the impact load tests.

3.3 *Test Results and Discussion.* Figure 13 shows typical stress-strain curves for the Oak material at vari-

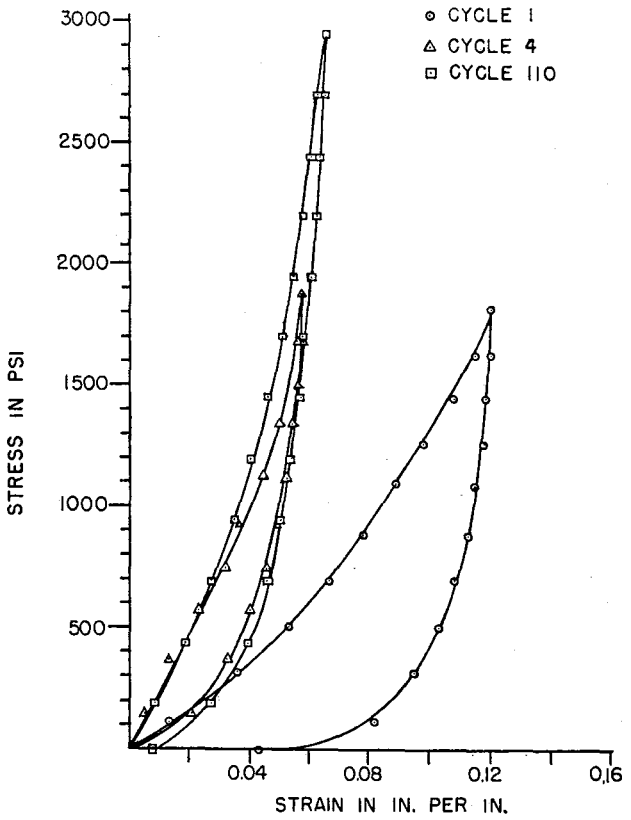


*Figure 14. Stress vs. strain for Garlock Asbestos cushion.*

ous loading cycles. It is noted that after approximately 10 cycles the stress-strain relationship becomes reasonably stable. Figure 14 shows similar stress-strain characteristics for the Garlock Asbestos material. This material has been used as cushioning on several occasions. It was believed to be able to withstand the driving energy and heat generated in a cushion without catching on fire as wood will often do.

Figure 15 shows the stress-strain relationship of the Micarta Plastic disks and also the characteristic stress-strain curve of the Micarta Capblock assembly which is usually composed of alternate layers of 1 in. thick Micarta Plastic disks and 0.5 in. thick aluminum disks. The Micarta Plastic and the Micarta Capblock assembly did not indicate any mechanical conditioning or permanent deformation under repeated cycles of load. Consequently their stress-strain characteristic remained essentially constant.

TABLE 7. SECANT MODULI OF ELASTICITY OF OAK WOOD CUSHIONING MATERIAL UNDER STATIC LOAD PERPENDICULAR TO GRAIN

| Stress Level in psi | Secant Modulus of Elasticity, $E_c$, in psi | | | |
|---|---|---|---|---|
| | Load Cycle 1 | Load Cycle 2 | Load Cycle 10 | Load Cycle 100 |
| 500 | 7,800 | 11,600 | 20,800 | 21,200 |
| 1000 | 10,400 | 17,000 | 28,600 | 29,400 |
| 1500 | 11,900 | 21,100 | 33,300 | 34,900 |
| 2000 | 13,100 | 23,300 | 37,000 | 39,300 |

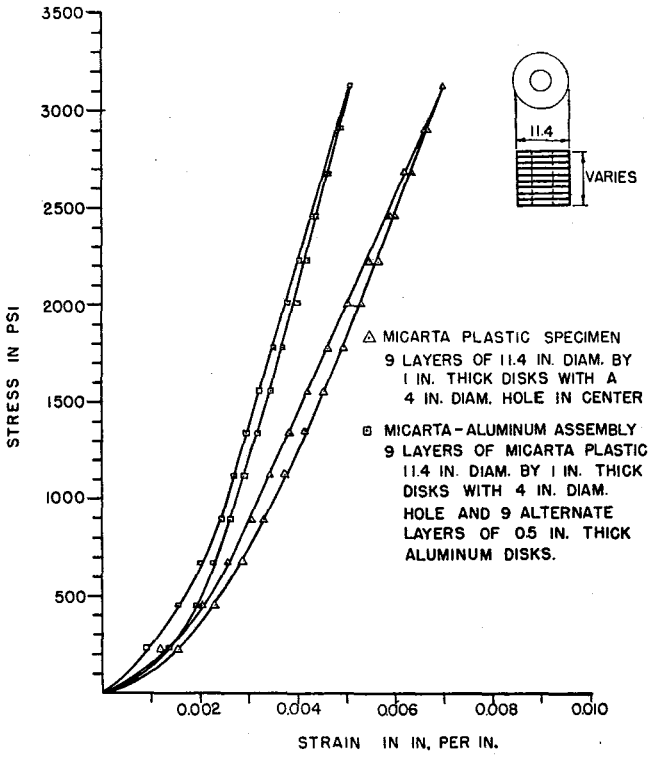


*Figure 15. Static stress vs. strain for Micarta Plastic and Micarta-Aluminum assembly.*

Tables 7 and 8 present a tabulation of Secant Moduli of Elasticity values for the Oak and Garlock Asbestos cushioning materials respectively. Values are given for different loading cycles and at different stress levels. Table 9 presents a tabulation of the Secant Moduli of Elasticity values for the Micarta and Micarta-Aluminum Assembly. Such values are useful when using Equations 1, 2, and 3 to calculate driving stress.

TABLE 8. SECANT MODULI OF ELASTICITY OF GARLOCK ASBESTOS CUSHIONING MATERIAL UNDER STATIC LOAD

| Stress Level in psi | Secant Modulus of Elasticity, $E_c$, in psi | | |
|---|---|---|---|
| | Load Cycle 1 | Load Cycle 4 | Load Cycle 110 |
| 500 | 9,430 | 23,800 | 23,800 |
| 1000 | 11,800 | 25,000 | 27,800 |
| 1500 | 13,900 | 28,300 | 31,900 |
| 2000 | | | 36,400 |
| 2500 | | | 41,400 |
| 3000 | | | 45,500 |

TABLE 9. SECANT MODULI OF ELASTICITY OF MICARTA AND MICARTA-ALUMINUM ASSEMBLY UNDER STATIC LOAD

| Stress Level in psi | Secant Modulus of Elasticity, $E_c$, in psi | |
|---|---|---|
| | Micarta | Micarta-Aluminum |
| 500 | 192,000 | 385,000 |
| 1000 | 299,000 | 455,000 |
| 1500 | 353,000 | 535,000 |
| 2000 | 385,000 | 588,000 |
| 2500 | 410,000 | 628,000 |
| 3000 | 435,000 | 653,000 |

# Chapter IV

## DISCUSSION OF WOOD STRUCTURE AND ANALYSIS OF ITS BEHAVIOR UNDER IMPACT LOAD PERPENDICULAR TO GRAIN

4.1 *The Structure of Wood.* Wood is composed predominantly of lignocellulose structures with various infiltrated substances. It can be divided into two broad classifications as follows:

1. Coniferous or evergreen species (softwoods such as Pine and Fir).

2. Deciduous species (hardwoods such as Oak and Gum).

These two classes differ not only in structure but also in chemical composition.[2] It is not the intention of this section however to explore in detail the composition of wood but only to present the rather elementary picture of its physical structure so as to give sufficient background for the discussions that follow.

4.2 *Microstructure.* The cell or tracheid is composed of minute distinct groups of cellulose called micelle. The micelle are approximately 50 A° units wide and 400 to 600 A° units in length. The micelle form into bundles about 3000 A° units thick to form the fibril.[3]

The cell wall is composed of an outer and inner shell. The outer shell is made up of a thin layer with the structural units (fibrils) orientated around the fiber at approximately right angles to the fiber direction. This layer is highly lignified and contains considerable hemicellulose (binder). The cellulose content of this wall is about 20 to 35 percent. The inner and much thicker shell is composed of fibrils spirally orientated and opposed in direction in adjacent layers.

The cells are cemented together by an intercellular substance or simple middle lamella which is largely lignin (80%) and hemicellulose (20%). A simple cell is on the order of 500,000 A° units in width. The length of the tracheids (cells) varies with the species with the longest measuring about 10 mm.[2]

4.3 *Macroscopic Structure.* As mentioned previously the structure of woods falls into two general classes, softwoods, and hardwoods.

Figure 16 is a sketch showing the structure of a typical softwood. The vertical cells are nearly all tracheids, mostly rectangular in cross-section and very uniform in size in the tangential direction (parallel to the annular rings). They are arranged in almost perfect radial lines and vary in size from very large and thin

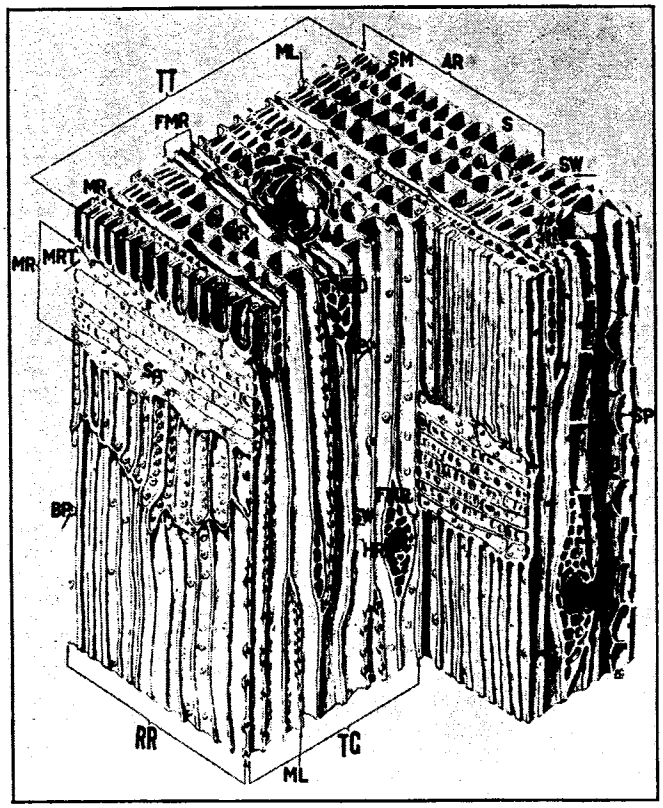


*Figure 16. Drawing of a block of Pine wood, greatly enlarged. TT, cross section; RR, radial section; MR, medullary ray; AR, annual ring; ML, middle lamella; SW, summer wood of previous growing season. (Courtesy of U. S. Forest Products Laboratory.)*

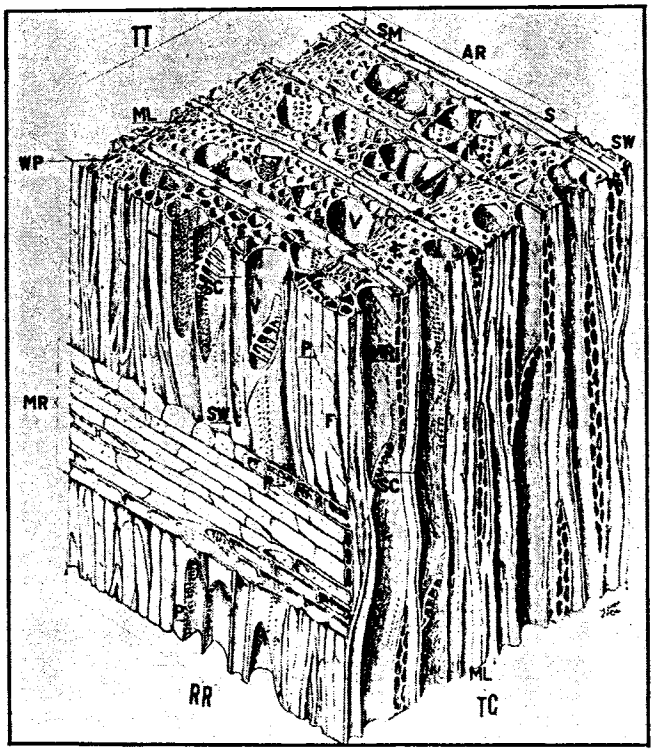


*Figure 17. Magnified three-dimensional diagrammatic sketch of a hardwood. TT, end grain surface; TG, tangential surface; RR, radial surface; F, fibers; V, vessels, or pores; SC, gratings of the vessels; P, pits; MR, wood ray; S, Springwood; SM, summerwood; AR, annual ring; ML, middle lamella: SW, summerwood of previous growing season; WP, wood parenchyma. (Courtesy of U. S. Forest Products Laboratory.)*

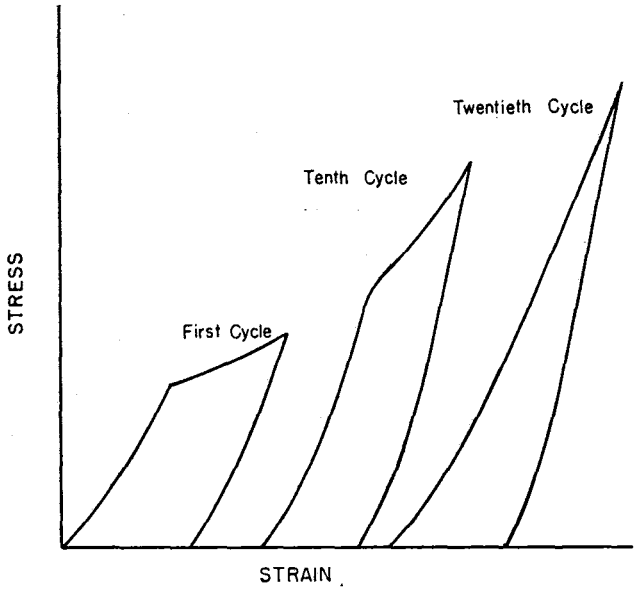


*Figure 18. Typical stress-strain curve for wood.*

walled in the earlywood to small and thick walled in the latewood. These cells (tracheids) are spliced for about one third of their length. Interspersed between these cells are the medullory or pith rays. These are very long, thin walled cells, perpendicular to the annular rings, and much shorter than the tracheids. These rays play a very important part in the discussion of the mechanics of fracture that follows. In most softwoods large vertical tubular openings occur between the cells. These are called resin ducts and are normally filled with resin. In general softwoods have a very ordered structure.[3]

Figure 17 shows a section of typical hardwood. Hardwoods are structurally more complex than soft woods. They consist of an unordered array of odd shaped vertical cells. The cells are usually shaped such that they form an interlocked matrix. In general the cells have much thicker walls than those in the softwoods. Interspersed within the cells are large diameter pores. These pores vary in size and spacing depending on the species. Medullary rays are present as in the softwoods. In general hardwoods are very dense structurally and have a higher specific gravity than do softwoods.[3]

4.4 *Behavior Under Impact Load Perpendicular to the Grain.* Figure 18 shows a typical stress strain curve for a softwood cushion at successive cycles of loading by a drop hammer.

Note that on the first cycle considerable yielding and permanent strain occurs. As the number of cycles is increased the wood hardens and eventually reaches a more stable state with the initial portions of the curve becoming more uniform. This phenomenon can be called mechanical conditioning. This can be visualized as the progressive breakdown of the large springwood cells due to a combination of flexural bending of the cell wall and shearing of the cell lattice (grid of cells) along the interface between the summerwood and springwood. Microscopic investigation reveals that the significant portion of the permanent deformation occurs in the springwood. No discernable permanent deformation is measurable in the latewood. Therefore it can be assumed that the material behaves as if it were composed of layers of elastic and plastic material, the plastic material exhibiting a work hardening characteristic.

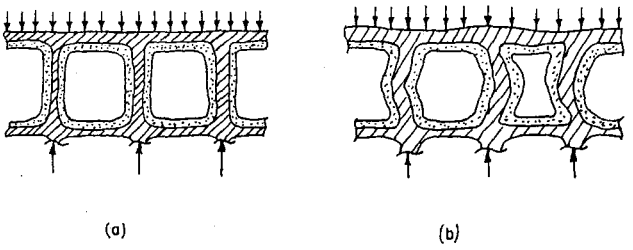


*Figure 19. Cells under axial load.*

The following observations are made on the mechanism of deformation and work hardening. The observations are based on microscopic examination of specimens that had been subjected to repeated impulsive loads perpendicular to the grain. It must be pointed out that these observations are solely those of the authors.

Consider the row of cells subject to an axial compression in Figure 19a.

The walls of each cell behave as a column and hence will have a critical buckling stress. When this stress is exceeded the wall will yield and possibly fracture. This is probably one of the reasons behind the progressive plastic deformation witnessed in the tests. It is noted that the walls are subject to shear stresses due to the complex state of stress in the deformed walls. Hence it is probable that some of the walls have shear failures which contribute to the deformation.

Consider now the case where the annular rings are inclined to the axis of the cushion as in Figure 20a. A small finite element "A" will be subject to the stress state shown in Figure 20(b).

Under this stress condition the earlywood cells will act in the manner of shear deformation as in Figure 20(c). Along the interface between the earlywood and latewood the bond between the adjacent cells will be broken down due to the localized tensile stresses normal to the interface. These stresses are due to the bending of the earlywood cell wall due to the shear effect. With the bond weakened locally a shear plane is developed. The fractured ends of the cell walls at the interface inter-

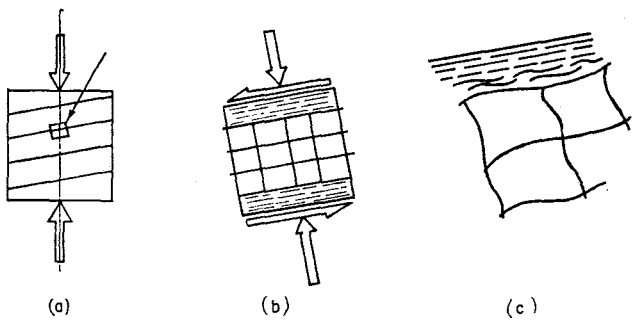


*Figure 20. Annular rings inclined to axis.*

lock and cause an increase in shear resistance for slip to occur. Presumably it is this interlocking which contributes to the mechanical conditioning or stabilizing of the stress-strain behavior.

The shear effect has been observed in the microscopic examination of the specimen. In a new piece of wood the medullary or pith rays are perpendicular to the annular rings. After repeated loadings these rays were observed to have assumed the characteristic S-shape of the shear deformation indicating the above discussed phenomenon.

At this stage of the investigation no conclusions have been made on the mechanical behavior of hardwoods. Their very unordered cell structure prohibits it.

# Chapter V

## SUMMARY OF CUSHION STUDY

Equations have been presented which will allow an engineer to determine the maximum compressive stress at a pile head during driving. Equations 1, 2, or 3 (whichever one is required by the problem) can be used to determine the desirable combination of ram weight, ram velocity, and cushion stiffness so as not to exceed a given allowable compressive stress at the head of a given pile. To use these equations or the computer solution of the wave equation reasonably accurate values of the Secant Modulus of Elasticity of various wood cushion materials are required. Such Secant Moduli values are tabulated in Tables 4, 5, 6, and 7 for Fir Plywood, Pine Plywood, Gum, and Oak respectively.

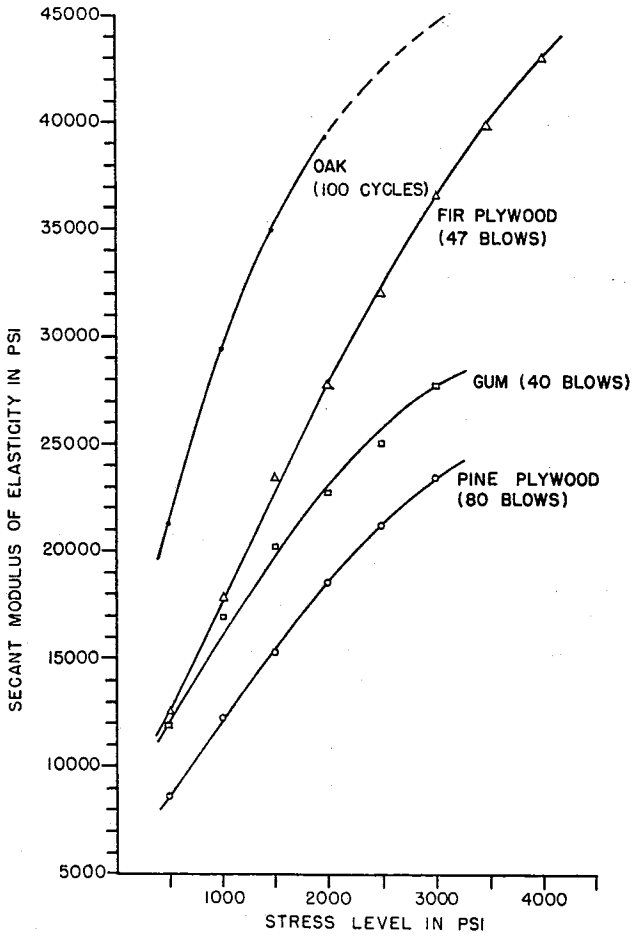


*Figure 21. Secant moduli of elasticity of various wood cushions vs. stress level.*

For practical pile driving problems in the field Secant Moduli of Elasticity values of the well consolidated cushions should be used, and not those from the 1st, 2nd, or 20th blow. Figure 21 shows the Secant Moduli of the well consolidated wood cushions for different stress levels. Since the area of the cushion will normally be the same as the area of the pile, the Secant Moduli will usually be chosen from Figure 21 to correspond with the maximum allowable stress level in the pile. For example, the secant moduli at a stress level of 2500 psi would be approximately

| | $E_c$ | u* |
|---|---|---|
| Pine Plywood | 21,200 psi | .27 |
| Gum | 25,000 psi | .20 |
| Fir Plywood | 32,100 psi | .43 |
| Oak | 43,000 psi | .50 |

*u values obtained from Figure 12.

The woods with the lower value of $E_c$ will allow a smaller cushion thickness and may seem more desirable. On the other hand the woods with the higher coefficient of restitution value u will deliver a larger percent of the driving energy to the pile and may give more pile penetration per blow.

The Green Oak, Gum, Pine Plywood, and Fir Plywood have been found to perform adequately as pile cushioning materials. The results of this investigation have shown however that each of these materials have their own characteristic values of elastic moduli and coefficients of restitution which must be considered in using various equations or formuli for predicting the dynamic behavior of piling.

## REFERENCE LIST


1. Hirsch, T. J., *A Report on Computer Study of Variables Which Affect the Behavior of Concrete Piles During Driving*, Texas Transportation Institute Report E 42-63, August 1963.
2. Stam, A. J., *Wood and Cellulose Science*, McGraw-Hill Book Co., New York, 1962.
3. Tiemann, H. D., *Wood Technology*, Pitman Publishing Corp., New York, 1951.
4. Thornton, D. L., *Mechanics Applied to Vibration and Balancing*, Chapman & Hall, London, 1951.